Low divergence electron beams from a gas cell

Contact: michael.backhouse13@imperial.ac.uk

M. P. Backhouse, R. Luo, J. Hills, L. Kennedy, C. Cobo, E. Los, Z. Najmudin
The John Adams Institute
Imperial College London
SW7 2BZ, United Kingdom

N. Lopes
GoLP/Instituto de Plasmas e Fusão Nuclear
Instituto Superior Técnico
1049-001 Lisboa, Portugal

E. Gerstmayr, J. Sarma
School of Mathematics and Physics
Queen's University Belfast
BT7 1NN, United Kingdom

N. Bourgeois, D. Bloemers, A. Thomas, S. Hawkes, S. Dann
Central Laser Facility
Rutherford Appleton Laboratory, Didcot
OX11 0QX, United Kingdom

Abstract

Reducing the divergence of LWFA-generated electron beams makes them better suited to many applications and to injection into subsequent acceleration stages. Here we report on the generation of electron beams with divergences below 0.2 mrad. The low divergence is achieved over a wide range of laser parameters and plasma densities, up to electron beam energies of 1.5 GeV. High-resolution image plate scans indicate that these measurements are overestimates and that the true beam divergence was lower than could be measured. The low divergence is attributed to the use of a gas cell target with a tailored exit aperture geometry.

1 Introduction

Laser wakefield accelerators typically produce electron beams with small source sizes, on the order of a micrometre, and large divergences, on the order of a few milliradian [1]. The transverse emittance, a measure of beam quality, is comparable to electron beams accelerated using conventional methods [2], but the large divergence causes the beam size to increase rapidly, resulting in emittance growth that is effectively irreversible. Significant emittance growth will make the beam unfocussable, such that injection into subsequent acceleration stages or undulators is ineffective [3, 4]. For other applications, such irradiating biological samples [5], a large divergence requires either beam optics or placing the sample close to the accelerator to maximise the current density of the beam, which may be impractical. Here, we report on the production of low-divergence electron beams using a gas cell with a specifically tailored exit aperture. The aperture confines the gas as it leaks out, producing a long density ramp that adiabatically damps the betatron motion of the electrons as they leave the plasma. These results have implications for future target design for applications where preserving the electron beam size and emittance is paramount.

2 Experimental Setup

The data reported here was obtained using the South beam of the Gemini laser system. An $f = 6$ m off-axis parabola focused the 150 mm diameter beam to a slightly elliptical spot. An ellipse fit to the half-maximum contour focal spot intensity had average major and minor radii ((24 ± 2) µm, (20 ± 1) µm), and contained $31\pm2\%$ of the energy. Here, the error denotes the standard deviation of the measurement. The target gas was helium doped with 2% nitrogen by weight. This was confined using a gas cell with

windows for probing the plasma. The pressure was monitored using sensors attached to the cell, and transverse interferometry was used to measure the plasma density immediately after its formation. The laser entered the cell through the tip of a nozzle, which could be translated to modify the length of the accelerator. The exit aperture was styled after a converging-diverging nozzle, with a 30° converging section and a 10° diverging section. The throat had a diameter of 1 mm and a length of 0.1 mm. This design accelerates the gas as it flows out of the cell, extending the scale length of the downramp.

The fringe fields in a dipole can cause electrons to be deflected transversely to the main dispersion direction. This is because the fringe fields must have a component that points along the optical axis to satisfy Maxwell's equations, and this will have a transverse focussing effect for electrons travelling at an angle to the z-axis. The magnitude of edge focusing in the dipole is approximately $f = -\rho/\tan\alpha$, where $\rho = p/(eB)$. For a 1 GeV, $\alpha = 1$ mrad beam in a 1 T dipole, $f = 1$ km so this effect is assumed to be negligible here.

The electron beam impinged on a Scintacor Luminex regular scintillating screen 1.4 m after the exit aperture of the gas cell. This screen was imaged onto a 12-bit CCD, allowing the transverse profile of the beam to be monitored. For spectral measurements, a 1 T 0.5 m long permanent dipole magnet could be translated onto the optical axis, which dispersed the beam onto other scintillating screens. These screens were placed at 1.7 m and 2.8 m after the exit aperture, and were imaged onto 16-bit sCMOS sensors. The polarisation of the laser was orthogonal to the dispersion plane. The absolute charge was calibrated using Fujifilm BAS-TR image plate placed on the spectrometer screens for a single shot. Transmission variations across the image were accounted for by imaging a constant source of green light at different places along the screen. The calibration was verified by comparing with the image plate measurement.

Kapton tape positioned 2−5 mm after the exit of the cell was often used to dump the laser.

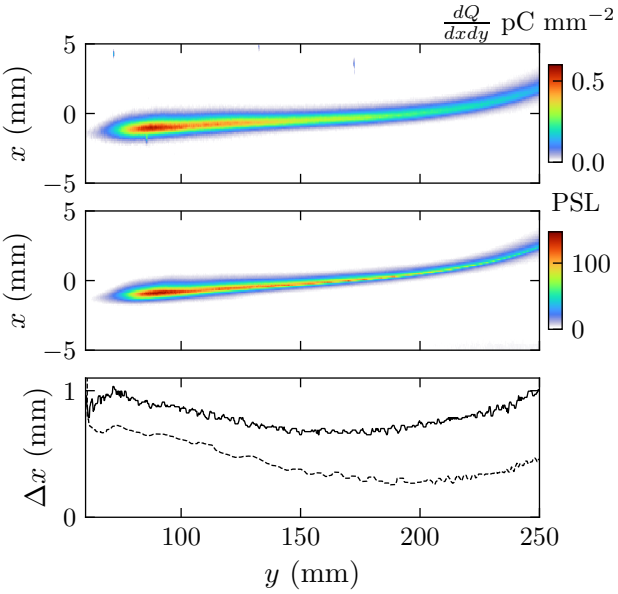

Figure 1: Comparison between the electron spectrometer and image plate measurements. Top: Image from the electron spectrometer. Middle: Scanned image plate from the same shot. Bottom: FWHM beam width as a function of position for the spectrometer (solid) and the image plate (dashed).

This increases beam divergence via elastic scattering; the 125 µm thick material has a calculated scattering angle of 0.2 mrad for 1 GeV electrons. To observe the unscattered beam the tape was not spooled, allowing a hole to form in the tape. This was the experimental configuration for the data reported here.

The measurements reported below overestimate the divergence when the resolution of the scintillating screen is considered. The Luminex medium used has a resolution of approximately 250 µm, which is close to the beam size on the screen of approximately 500 µm. To illustrate this, in Fig. 1 we compare an image from the electron spectrometer to the scanned image plate from this shot, which was used for the charge calibration. The y axis is the dispersion direction and the z axis is the beam axis. This shot was taken with the Kapton tape in the beam, so the divergence is higher than in the measurements made without the

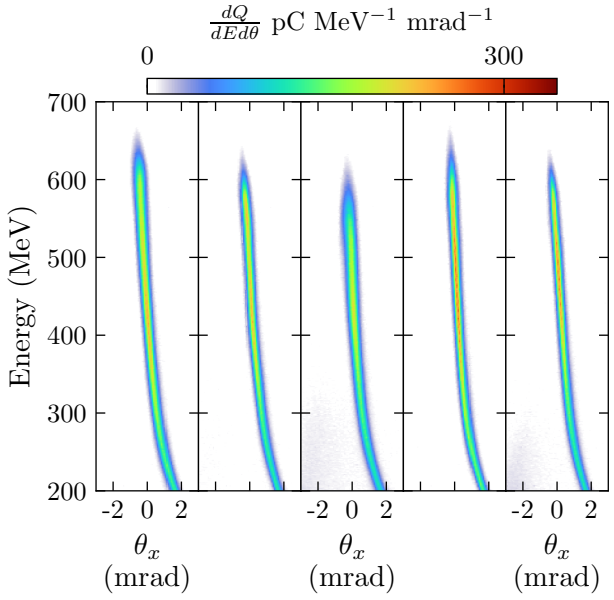

Figure 2: Sequential electron beam spectra highlighting the low divergence of the beams.

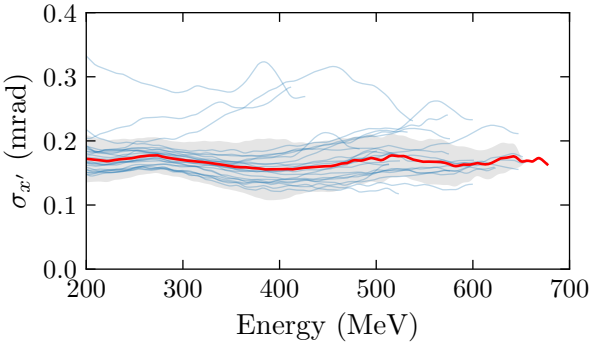

Figure 3: Energy resolved divergence measurements for the run containing the shots displayed in Fig. 1. The blue lines are the measurements for each spectrum in the data set, the red line is the median, and the shaded region is the standard deviation.

tape present. The width of the beam at its narrowest is 180 µm, whereas the beam width in the images at this point is over double this size. Given the 1.7 m distance from the source, this equates to a minimum Gaussian divergence of $\sigma_{x'} = 0.04$ mrad.

In principle, these measurements could be used to estimate the true beam divergence on all shots. However, scattering in the image plate and surrounding protective foils also increases the beam size once it hits the spectrometer screen due to the small but finite distance between them. Since this distance between the image plate and the scintillator screen is not known precisely the deconvolution would be exposed to a significant source of error. Consequently, the divergence measurements reported below have been left unadjusted.

3 Experimental Results

Fig. 2 shows processed images from the electron spectrometer. During these shots the mean laser energy was (8.2 ± 0.3) J, giving a peak intensity of $(5.6 \pm 0.6) \times 10^{18}$ W cm^{-2}, or $a_0 = (1.6 \pm 0.1)$, the internal cell length was 6.9 mm, and the plateau plasma density was $(2.7 \pm 0.2) \times 10^{18}$ cm^{-3}. Laser energy and plasma length were deliberately set to limit the peak energy of the electron beam and enhance shot-to-shot stability; operating at reduced laser energy provided margin for decreases in laser energy throughout shooting. At lower energies, the beam appears to point in the positive θ_x direction. The source of this deflection is currently unknown, with possible explanations being a steering effect due to transverse asymmetries in the gas flow, or fringe fields in the dipole magnet.

For each spectrum, the divergence of the beam in the x direction was determined by measuring the FWHM of the profile as a function of energy, scaled to the equivalent Gaussian width, $\sigma_{x'}$. These measurements are reported in Fig. 3, which shows that across the spectrum the median measured divergence did not exceed 0.2 mrad, with an average total divergence of (0.17 ± 0.03) mrad, where the error is the mean standard deviation over all shots. The mean charge for this dataset was (90 ± 10) pC.

Example electron beam profile measurements are shown in Fig. 4, taken immediately after the measurements in Fig 2. The x direction is the same as the x direction in Fig 2.

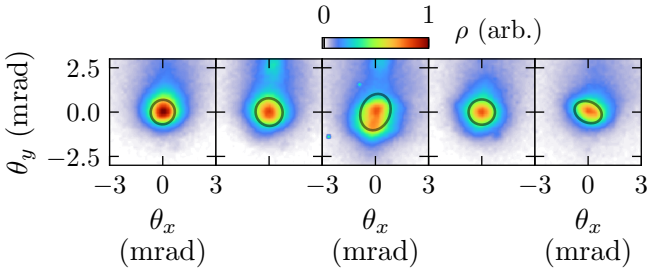

Figure 4: Electron beam profile example images using the same parameters as the shots in Fig. 2. The black line is an ellipse fit to the FWHM contour of the beam.

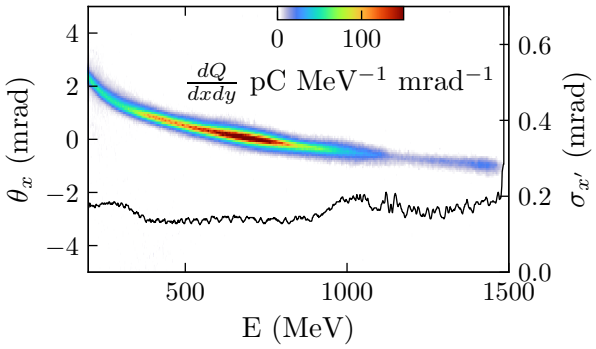

Figure 5: Example shot using more laser energy, demonstrating higher electron energies with low divergence.

The mean major and minor ellipse widths were (1.6±0.1) mrad and (1.4±0.1) mrad respectively, and the angle of the ellipse to the x axis was slightly biased towards 0. A slight asymmetrical elongation of the beam profile in the positive y direction was sometimes observed, as seen in the second and third electron beam profile examples. This was attributed to the magnet's proximity owing to the skew's sensitivity to the magnet position, and could not be completely removed due to limited magnet travel range. The beam divergence measurements from the profile diagnostic are higher than those from the spectrometer. This discrepancy can be explained by considering the effect of low-energy electrons, which typically have a larger divergence due to their lower longitudinal momentum. Since the profile diagnostic integrates across all energies, these low-energy electrons increase the average divergence.

A small number of shots were taken with higher laser energy of (11.2 ± 0.2) J and without the tape being translated between shots, allowing the divergence of higher-energy electron beams to be measured. Fig. 5 shows a typical shot from this dataset, where the peak energy of the electron beam exceeded 1.4 GeV. The beams generated in this regime exhibited lower shot-to-shot stability and had different spectra to those generated using the laser parameters for the data in Fig. 2. The sub-0.2 mrad divergence was consistent with the measurements at lower energy, indicating that the low divergence is relatively intensive to input parameter variability.

4 Discussion

The divergence measurements presented above should be viewed in the context of the transverse resolution limit of the spectrometer, captured in Fig. 1. Divergence measurements below 0.2 mrad are being overestimated by a factor of 2 or more, indicating that electron beams with divergences below 0.1 mrad are being generated.

These measurements are similar to the state-of-the-art in LWFA, such as those reported in [6], where the beam was then used to seed an x-ray free-electron laser. More comparable results are given in [7], where a gas cell target was used with the Gemini laser to accelerate electrons to high energies with 0.5−1 mrad divergences. The gas cell used in that experiment had a smaller exit aperture diameter than the one used here, and the shape of the aperture differed by having no converging section and a more oblique diverging section. We attribute the divergence improvements to the extended downramp scale-length, which adiabatically damps the electron betatron motion before leaving the plasma.

In the context of capturing charge in a second acceleration stage without coupling optics, a low divergence is advantageous because it reduces the beam size at the next stage, or allows stages

to be separated further. This can be advantageous since it provides more space for coupling optics. Emittance growth in the drift space is also subdued, since ${\epsilon_n}^2 = \bar{\gamma}^2({\sigma_\gamma}^2 z^2 {\sigma_{x'}}^4 + {\epsilon_0}^2)$, where ϵ_n is the normalised x projected emittance, $\bar{\gamma}^2$ is the mean Lorentz factor of the beam, σ_γ is the energy spread, z is the propagation distance and ϵ_0 is the initial emittance [8]. For a 1% energy spread beam with an initial emittance of 200 nm, corresponding to an 2 µm beam size at the accelerator exit, the emittance growth in an 10 mm drift space for a 0.1 mrad beam would be 2 %. For a divergence of 1 mrad, the growth would be 200 %. Due to the technological importance of generating beams with high transverse beam quality via LWFA, we continue to explore the mechanisms for their generation.

The authors acknowledge: STFC funding (ST/J002062/1, ST/P002021/1, ST/V001639/1), and the CLF's technical support.

References

[1] S. Kneip et al., *Physical Review Special Topics - Accelerators and Beams*, **15**, 021302 (2012)
[2] C. M. S. Sears et al., *Physical Review Special Topics - Accelerators and Beams*, **13**, 092803 (2010)
[3] S. Steinke et al., *Nature*, **530**, 190 (2016)
[4] W. Wang et al., *Nature*, **595**, 516 (2021)
[5] V. Malka et al., *Mutation Research/Reviews in Mutation Research*, **704**, 142–151 (2010)
[6] L. T. Ke et al., *Physical Review Letters*, **126**, 214801 (2021)
[7] K. Poder et al., *Physical Review Letters*, **132**, 195001 (2024)
[8] M. Migliorati et al., *Physical Review Special Topics - Accelerators and Beams*, **16**, 011302 (2013)